Cosmic Research, Vol. 37, No. 1, 1999, pp. 34–39. Translated from Kosmicheskie Issledovaniya, Vol. 37, No. 1, 1999, pp. 38–43.

Shape and Location of Planetary Bow Shocks

M. I. Verigin,[1] G. A. Kotova,[1] A. P. Remizov,[1] V. A. Styazhkin,[1] N. M. Shutte,[1] T.-L. Zhang,[2] W. Riedler,[2] H. Rosenbauer,[3] K. Szegö,[4] M. Tatrallyay,[4] and K. Schwingenschuh[2]

[1] *Space Research Institute, Russian Academy of Sciences, ul. Profsoyuznaya 84/32, Moscow, 117810 Russia*
[2] *Institut für Weltraumforschung, Graz, Austria*
[3] *Max-Planck-Institut für Aeronomie, Katlenburg-Lindau, Germany*
[4] *Central Research Institute for Physics, Budapest, Hungary*

Received February 4, 1997

Abstract—We developed a semiempirical quantitative model of a planetary bow shock, which describes variations in its location and shape caused by variations in parameters of the solar wind flow and in the shape of the obstacle (magnetopause). Based on this model, we explore the near-Mars bow shock, the experimental data of which were obtained on the *Phobos-2* spacecraft. Unusual properties of near-Mars bow shock are analyzed.

INTRODUCTION

Plasma (TAUS) and magnetic (MAGMA) experiments carried out on board the *Phobos-2* spacecraft, which operated for about two months in orbit around Mars, presented a great body of data on intersections of the Martian bow shock. Analysis of these data made it possible to reveal unusual properties of the bow shock near Mars, as compared to the properties of bow shocks observed previously near other planets. On the one hand, the dispersion of the observed locations of the Martian bow shock near the terminator plane was found to be very large [1], which is typical of bow shocks near the planets whose magnetospheres are produced by their intrinsic magnetic fields. Furthermore, the location of the bow shock close to the terminator near Mars depends very slightly on the solar wind dynamic pressure ρV^2 (where ρ is the density and V is the speed of the solar wind plasma) [1, 2], but rather depends on the angle θ_{bn} between the direction of the interplanetary magnetic field and the normal to the bow shock [3]. This is similar to the bow shock observation near Venus, the planet having no intrinsic magnetic field [4].

Verigin *et al.* [1] explained these unusual properties of the Mars bow shock assuming that the location of the boundary of the obstacle to the solar wind flow (the magnetopause) in the subsolar region is rather stable. In the next paper [5] the authors developed a quantitative model of the Martian magnetopause. The specific feature of this model magnetopause is that its shape varies with the solar wind dynamic pressure, whereas the location in the subsolar region is almost stable for $\rho V^2 \geq 6 \times 10^{-9}$ dyn cm^{-2}.

In this paper we consider a semiempirical quantitative bow shock model whose parameters are the characteristics of the solar wind (ρV^2, θ_{bn}, the Alfvenic M_A and sonic M_s Mach numbers), as well as the shape and location of the magnetopause. The observed locations of the bow shock of Mars are compared to the model locations calculated according to the model of the Martian magnetopause and solar wind parameters measured at each orbit of *Phobos-2* around Mars.

CONSTRUCTION OF THE BOW SHOCK MODEL AND COMPARISON WITH PREVIOUS MODELS

Modeling of planetary bow shocks was begun with the hydrodynamic calculations performed by Spreiter *et al.* [6] who examined the flow past an obstacle whose shape is similar to the Earth's magnetosphere ($R_0/r_0 \approx 1.26$, where R_0 is the radius of the curvature of the obstacle—magnetopause—and r_0 is the distance from the planet's center to the obstacle's subsolar point). These calculations were carried out for several values of the sonic Mach number M_s and an adiabatic exponent γ. Spreiter *et al.* [6] assumed that the ratio of the distance Δ between the bow shock and magnetopause to r_0 depends only on the density discontinuity at the bow shock ε:

$$\Delta/r_0 = 1.1\varepsilon, \qquad 5 < M_s < \infty, \tag{1}$$

where

$$\varepsilon = \rho_1/\rho_2 = [(\gamma-1)M_s^2 + 2]/[(\gamma+1)M_s^2] \tag{2}$$

(subscripts 1 and 2 refer to the plasma flow upstream and downstream of the bow shock, respectively). In the subsequent calculations Farris and Russell [7] revised intuitively relationship (1) bearing in mind that the condition $\Delta \longrightarrow \infty$ must be satisfied when $M_s \longrightarrow \infty$:

$$\Delta/r_0 = 1.1\varepsilon M_s^2/(M_s^2 - 1). \tag{3}$$

Finally, modern computers made it possible to perform the magnetohydrodynamic calculations of the flow past the magnetosphere ($R_0/r_0 \approx 1.47$) [8], but again for the limited number of values of M_s, M_A, and

0010-9525/99/3701-0034$22.00 © 1999 МАИК "Наука/Interperiodica"

θ_{bn}. The results of these calculations are approximated by the dependence

$$\Delta/r_0 = 3.4\varepsilon - 0.6, \quad M_s = 7.6, \quad 1.4 < M_A < \infty, \quad (4)$$

where ε is now the real root of the cubic equation (see, for example, [9]):

$$\varepsilon^2 - \left(\frac{\gamma-1}{\gamma+1} + \frac{\gamma + (\gamma+2)\cos^2\theta_{bn}}{(\gamma+1)M_A^2} + \frac{2}{(\gamma+1)M_s^2}\right)\varepsilon^2 + \frac{1}{(\gamma+1)M_s^2}\left(\gamma(1+\cos^2\theta_{bn}) - 2 + \cos^2\theta_{bn}\right. \quad (5)$$

$$\left.\times\left(\frac{\gamma+1}{M_A^2} + \frac{4}{M_s^2}\right)\right)\varepsilon - \frac{\cos^2\theta_{bn}}{(\gamma+1)M_A^4}\left(\gamma - 1 + \frac{2\cos^2\theta_{bn}}{M_s^2}\right) = 0.$$

Generally speaking, gas dynamic calculations of the flow past bodies of various shape were made long before the calculations for the planetary magnetospheres. Out of many existing approximations, the expression for Δ obtained by Minailos [10]:

$$\Delta/r_0 = \varepsilon(0.76 + 1.05\varepsilon^2), \quad 1.5 < M_s < \infty; \quad (6)$$

and the expression for the radius R_s of the bow shock curvature obtained by Stulov [11]:

$$R_s = \Delta(1 + \sqrt{8\varepsilon/3})/\varepsilon, \quad M_s \geq 3 \quad (7)$$

are worth noting. Of some interest are the analytical studies of the asymptotic behavior of R_s and Δ at $M_s \longrightarrow 1$ performed by Shugaev [12]:

$$\Delta \sim (M_s - 1)^{-2/3}, \quad (8)$$

$$R_s \sim (M_s - 1)^{-5/3}. \quad (9)$$

Figure 1 shows the parameter Δ/r_0 as a function of the quantity $\xi = \varepsilon/(1-\varepsilon)$ according to the data of gas dynamic experiments (see, for example, the data summarized by Belotserkovskii *et al.* [13] on the flow past a sphere ($r_0 = R_0$)). Short and long dashes in this figure show dependences (6) and (8), respectively. All these data can be fitted with the relation:

$$\Delta/r_0 = (R_0/r_0)(\xi/(1.87 + 0.86/\xi^{3/5}))^{2/3}, \quad (10)$$

which describes correctly the dependence sought in the entire range of sonic Mach numbers (Fig. 1a, solid line). Similarly, the dependence of the parameter R_s/r_0 on ξ (Fig. 1b, solid line) can be approximated by the relation

$$R_s/r_0 = (R_0/r_0)((1.058 + \xi)/1.067)^{5/3}, \quad (11)$$

which is a good fit to the results of gas dynamic experiments for medium Mach numbers, and approaches asymptotically expressions (7) and (9) for high and low Mach numbers, respectively.

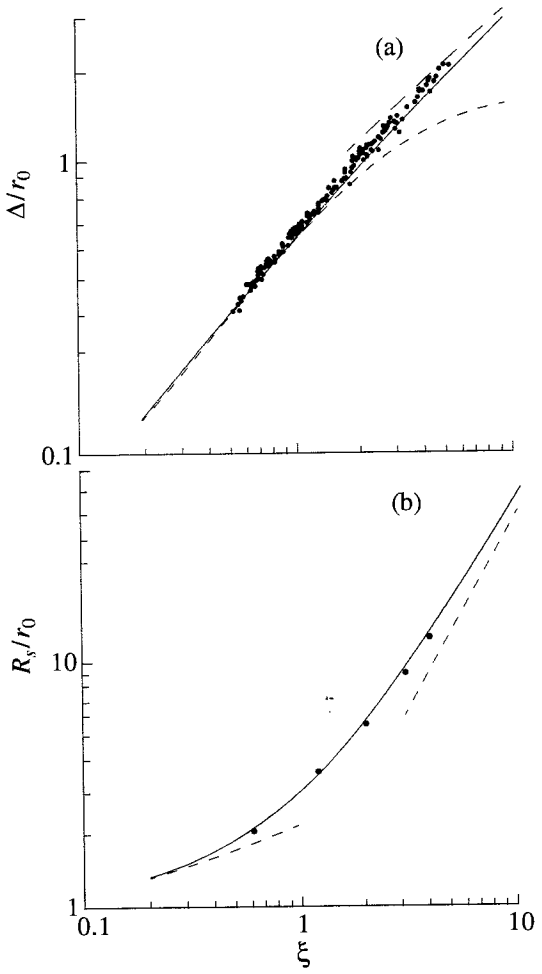

Fig. 1. Determination of the empirical dependence of the parameters Δ/r_0 (a) and R_s/r_0 (b) on the quantity $\xi = \varepsilon/(1-\varepsilon)$. The long-dashed line in (a) corresponds to dependence (8); the short-dashed lines, to dependence (6). In the case (b) the upper and lower dashed lines correspond to formulas (9) and (7), respectively.

Let us compare the relations obtained above to the results of hydrodynamic and magnetohydrodynamic calculations of flow past the Earth's magnetosphere. The solid line in Fig. 2a shows the relation between Δ/r_0 and M_s, which corresponds to Eq. (10). Good agreement is seen with the results of the latest calculations made by Spreiter and Stahara [14] (dots), including the M_s values lower than those in the previous paper [6]. The long-dashed line corresponds to empirical relation (1) [6], which underestimates the Δ value for low Mach numbers, whereas relation (3) [7] (short-dashed line) overestimates Δ for low M_s.

Figure 2b shows the relation between Δ/r_0 and M_A according to Eq. (3) for $M_s = 7.6$. Here relationship (5) was used for calculating ε and ξ. The results of the magnetohydrodynamic calculations [8] are presented by dots and squares for $\theta_{bn} = 90°$ and 45°, respectively. It is evident from Fig. 4 that relationship (10) is also in

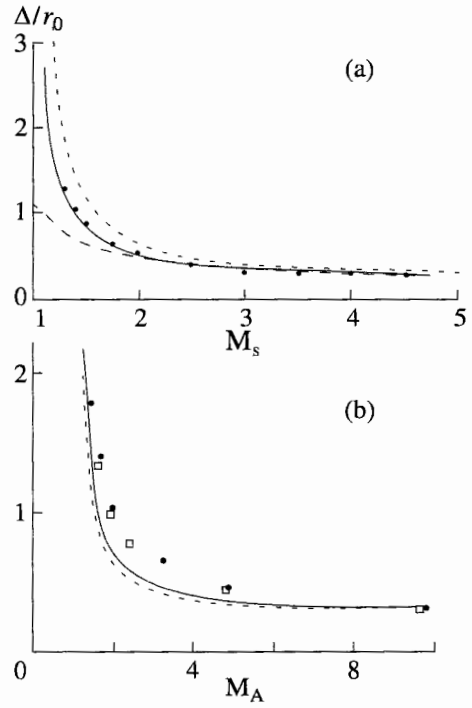

Fig. 2. Comparison of the empirical dependences (10) and (11) with the results of hydrodynamic (a) and magnetohydrodynamic (b) calculations. The solid line in (b) is calculated from Eq. (11) at $\theta_{bn} = 90°$, the dashed line corresponds to $\theta_{bn} = 45°$.

reasonable agreement with the results of magnetohydrodynamic calculations of flow past the magnetosphere.

As a zero approximation, the planetary bow shock can be described in the cylindrical coordinates (the x-axis is directed from the planet's center toward the Sun and y is the distance from this axis) by a certain hyperbolic curve. To determine this curve, it is necessary and sufficient to know these three parameters: the minimum distance (at the subsolar point) from the obstacle to the bow shock, the radius of the bow shock curvature, and its asymptotic behavior at large distances from the obstacle downstream of the flow. We denote by $\theta = \arcsin(1/M)$ the angle between the bow shock direction at infinity and the Sun–planet line, where $M_{ms} \le M \le \min(M_A, M_s)$ and $M_{ms} = (1/M_A^2 + 1/M_s^2)^{-1/2}$ is the magnetosonic Mach number. The hyperbola equation can then be written as

$$x = r_0 + \Delta + R_s(M^2 - 1) - R_s(M^2 - 1)\sqrt{1 + y^2/[R_s^2(M^2 - 1)]}. \quad (12)$$

The next approximation for determining the shape of the bow shock may be the curve, which retains the useful properties of hyperbola (12) but involves an additional parameter χ, which enables one to approximate the results of the hydrodynamic calculations [14, 15]:

$$x = r_0 + \Delta + \chi R_s(M^2 - 1) - \frac{1}{2}(1 - \chi)\sqrt{(M^2 - 1)} - \chi R_s(M^2 - 1)\sqrt{1 - \frac{y(1-\chi)}{\chi R_s\sqrt{(M^2-1)}} + \frac{y^2(1+\chi)^2}{4\chi^2 R_s^2\sqrt{(M^2-1)}}}. \quad (13)$$

To provide agreement between the model bow shock and the results of the hydrodynamic calculations by Spreiter *et al.* [14, 15] we used the parameter

$$\chi = 0.38R_0/r_0 - 0.47 + 3.63/\gamma^2 - 3.51(1 - \varepsilon)/\varepsilon. \quad (14)$$

The present calculations based on formula (13), with the use of (14), are compared in Fig. 3 with the hydrodynamic calculations of the shape and location of the bow shock made by Spreiter *et al.* (a) for the obstacle of a constant shape, such as the Earth's magnetosphere ($R_0/r_0 = 1.26$) [14] and (b) for the obstacle of a variable shape, such as the Venus magnetosphere ($R_0/r_0 = (1 + \sqrt{1 + 8H/r_0})/2$, where H is the scale of the ionosphere height) [15]. Dots and solid lines in Fig. 3a are calculated for $\gamma = 5/3$; triangles and dashed lines correspond to $\gamma = 2$; the calculation for each γ was made for three values: $M_s = 2$, 4, and 8. As M_s increases (at constant γ), the bow shock approaches the obstacle. In Fig. 3b, the calculations are carried out for different H/r_0 ratios at $\gamma = 5/3$ and $M_s = 8$. We see that the model examined in the present study agrees well with the previous hydrodynamic calculations.

BOW SHOCK NEAR MARS

To calculate the location of the Martian bow shock, we used the parameters of the undisturbed solar wind: the proton density n_p, velocity V, and temperature T_p, as measured in the TAUS experiment, and the magnetic field **B** measured with the MAGMA magnetometer on board the *Phobos-2* spacecraft. Using these parameters, the quantities ρV^2, M_s, and M_A were calculated by the method described in [5]. Unfortunately, because of the spacecraft rotation, at most orbits around the planet only the absolute value of the magnetic field B and its components along and perpendicular to the Sun–Mars line can be used for reliable analysis. This circumstance makes no difference for calculating the angle θ_{bn} in the subsolar region. Its influence on the choice of the M value determining the asymptotic behavior of the bow shock at large distances from the planet leads to the scatter of the calculated intersections of the bow shock with the *Phobos-2* spacecraft orbit, which is much less than the scatter in experimental locations of the bow shock. For definiteness, we used the value $M = M_{ms}$. The quantity ρV^2 is the input parameter for constructing the magnetopause model (the value of the Martian intrinsic magnetic moment was taken to be 0.82×10^{22} G cm^3) [5] and, therefore, for determining the subsolar distance from

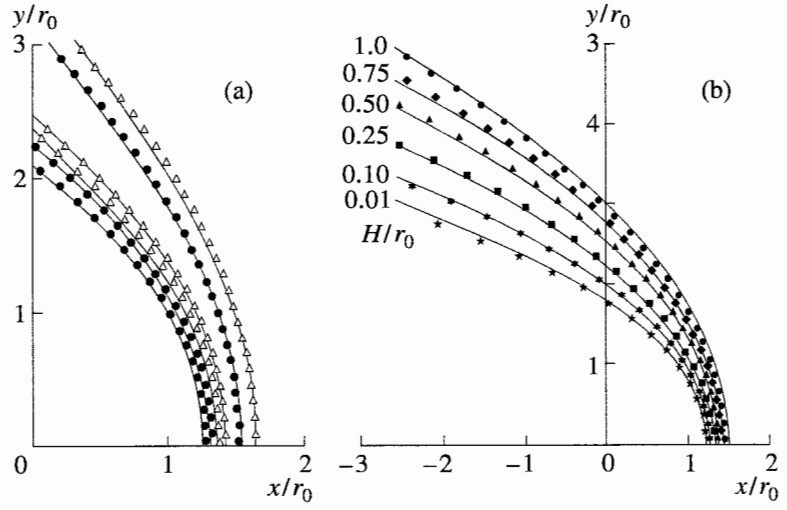

Fig. 3. Comparison of the shape and location of the planetary bow shock calculated from empirical relation (13) (various symbols) with hydrodynamic calculations (solid and dashed lines).

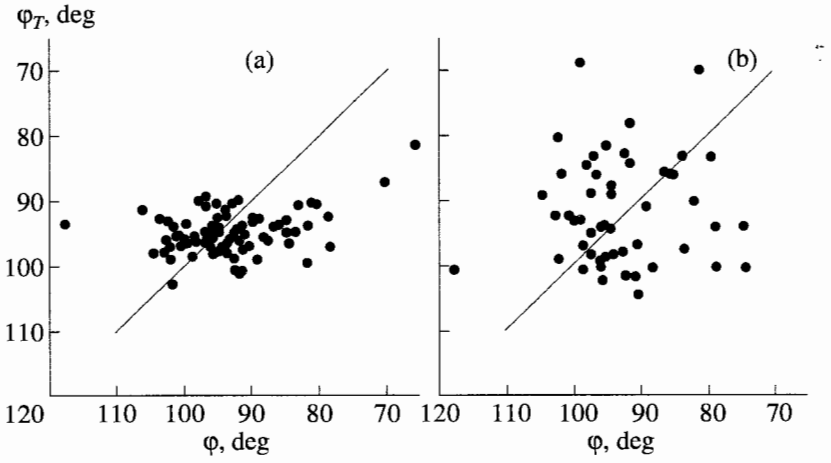

Fig. 4. Comparison of zenith angles for the calculated locations of the bow shock with those observed on the *Phobos-2* spacecraft. The straight lines correspond to the coincidence of these zenith angles. In cases (a) and (b) different methods of calculation were used (see text).

the planet's center r_0 to the magnetopause and its radius of curvature R_0. Thus, a knowledge of the quantities ρV^2, M_s, M_A, and θ_{bn} makes it possible to construct the model of the bow shock near Mars according to Eq. (13) and calculate the expected zenith angles for the sites of intersection of the Martian bow shock with the circular orbit of *Phobos-2*.

In Fig. 4a the calculated locations of the bow shock (the calculated zenith angles φ_T) are compared to those observed on the *Phobos-2* spacecraft (the observed zenith angles φ). In these calculations we used $\gamma = 2$. The use of the value $\gamma = 5/3$ increases the calculated zenith angles by about 5°. General agreement between the calculated and observed locations of the bow shock is evident, but the scatter of the calculated locations is much smaller than that of the observed values. The reason is probably connected with time variations of the solar wind parameters, because the parameters of the undisturbed solar wind were measured about half an hour before or half an hour after the crossing of the bow shock by the spacecraft and, therefore, they are offset by about one and a half hours in time from the intersection of the magnetopause. For this reason, the locations of the bow shock were also calculated by the alternative method (Fig. 4b); we used the theoretical values of the dynamic pressure and, accordingly, the corrected values of M_s and M_A of the solar wind corresponding, according to the existing model [5], to the recorded intersections of the magnetopause. The scatter of the measured and thus calculated locations of the bow shock is approximately the same (Fig. 4b), which supports the considerable influence of time variations of

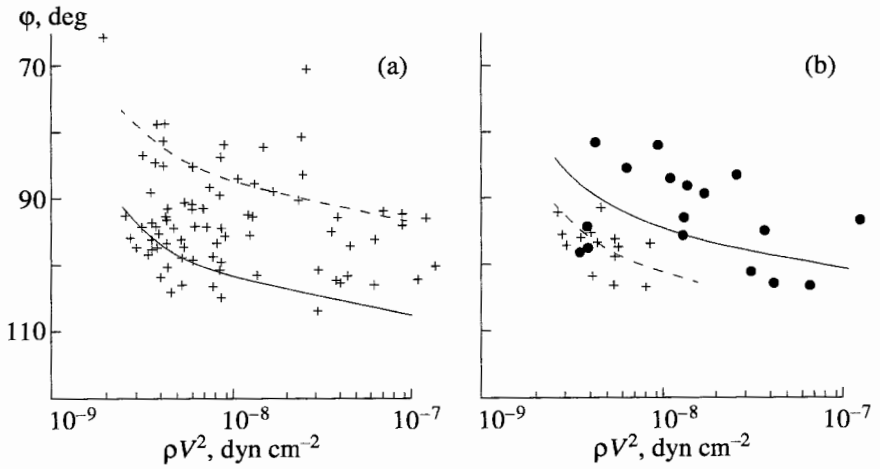

Fig. 5. (a) Comparison of the observed and calculated dependences of the location of the Martian bow shock on the solar wind dynamic pressure and (b) the dependence of the Martian bow shock location on the solar wind dynamical pressure in the narrow ranges of Mach numbers. Dots correspond to Mach numbers in the ranges: $4 < M_s < 6$, $5 < M_A < 8$. Crosses correspond to Mach numbers in the range $6 < M_s < 10$, $8 < M_A < 12$.

the solar wind parameters on the scatter of locations of the Martian bow shock.

In Fig. 5a we examine the dependence of the zenith angle for the observed intersections of the bow shock of Mars on the dynamic pressure of the undisturbed solar wind. The solid and dashed lines shown in this figure were calculated from Eq. (13). The calculations were made for $M_s = M_A = 10$, $\theta_{bn} = 0°$, and for $M_s = M_A = 4$, $\theta_{bn} = 90°$, respectively. Both curves correspond to the weak dependence of the calculated locations of the bow shock on the solar wind dynamic pressure, in accordance with observations. This confirms the validity of the proposed model of the bow shock.

In Fig. 5b we present two data sets of intersections of the Martian bow shock selected in the limited ranges of Mach numbers of the undisturbed flow. The theoretical curves calculated for medium Mach numbers (the solid curve for $M_s = 5$, $M_A = 6.5$, $\theta_{bn} = 0°$ and the dashed curve for $M_s = 8$, $M_A = 10$, $\theta_{bn} = 90°$) describe rather well the observational results in these cases too.

CONCLUSIONS

(1) We developed an empirical model for the planetary bow shock, which describes reasonably well the variations of its location and shape with the parameters of the undisturbed plasma flow (ρV^2, M_s, M_A, θ_{bn}) and the variations of the shape of the magnetopause (R_0, r_0).

(2) This model enables one to account for some unusual properties of the Martian bow shock.

(3) Some cases of observation of planetary bow shocks at unusually low Mach numbers (see, for example, [16, 17]) can be analyzed with the aid of the presented model.

ACKNOWLEDGMENT

This work is supported by the Russian Foundation for Basic Research (project no. 95-02-04223) and the INTAS grant no. 94-982.

REFERENCES

1. Verigin, M.I., Gringauz, K.I., Kotova, G.A., *et al.*, The Dependence of the Martian Magnetopause and the Bow Shock on Solar Wind Ram Pressure according to Phobos 2 TAUS Ion Spectrometer Measurements, *J. Geophys. Res.*, 1993, vol. 98, p. 1303.
2. Schwingenschuh, K., Riedler, W., Zhang, T.-L., *et al.*, The Martian Magnetic Field Environment: Induced or Dominated by Intrinsic Magnetic Field?, *Adv. Space Res.*, 1992, vol. 12, p. (9)213.
3. Zhang, T.-L., Schwingenschuh, K., Russell, C.T., and Luhmann J.G. Asymmetries in the Location of the Venus and Mars Bow Shock, *Geophys. Res. Lett.*, 1991, vol. 18, p. 127.
4. Tatrallyay, M., Russell, C.T., Mihalov, J.D., and Barnes, A., Factors Controlling the Location of the Venus Bow Shock, *J. Geophys. Res.*, 1983, vol. 88, p. 5613.
5. Verigin, M., Apathy, I., Kotova, G., *et al.*, Dependence of Martian Magnetopause Shape and Its Dimensions on Solar Wind Dynamic Pressure according to *Phobos-2* Data, *Kosm. Issled.*, 1996, vol. 34, no. 6, pp. 595–603.
6. Spreiter, J.R., Summers, A.L., and Alksne, A.Y., Hydromagnetic Flow around the Magnetosphere, *Planet. Space Sci.*, 1966, vol. 24, p. 223.
7. Farris, M.H. and Russell, C.T., Determining the Standoff Distance of the Bow Shock: Mach Number Dependence and Use of Models, *J. Geophys. Res.*, 1994, vol. 99, p. 17681.
8. Cairns, I.H. and Lyon, J.G., MHD Simulations of the Earth's Bow Shock at Low Mach Numbers: Standoff Distances, *J. Geophys. Res.*, 1995, vol. 100, p. 17173.

9. Zhuang, H.C. and Russell, C.T., An Analytic Treatment of the Structure of the Bow Shock and Magnetosheath, *J. Geophys. Res.*, 1981, vol. 86, p. 2191.
10. Minailos, A.V., Similitude Parameters and Approximating Dependencies of Axial-Symmetric Hypersonic Flow around Ellipsoids, *Izv. Akad. Nauk SSSR, Mekh. Zhidk. Gaza*, 1973, no. 3, p. 176.
11. Stulov, V.P., On the Similitude Law at Hypersonic Flow around Obtuse Bodies, *Izv. Akad. Nauk SSSR, Mekh. Zhidk. Gaza*, 1969, no. 4, p. 142.
12. Shugaev, F.V., Axial-Symmetric Flow Far from a Body and Near to the Axis for the M_∞ Number Close to Unity, *Prikl. Mat. Mekh.*, 1964, no. 1, p. 184.
13. Belotserkovskii, O.M., Bulekbaev, A., Golomazov, M.M., *et al., Obtekanie zatuplennykh tel sverkhzvukovym potokom gaza (teoreticheskoe i eksperimental'noe issledovaniya)* [Hypersonic Gas Flow around Obtuse Bodies (Theoretical and Experimental Studies)], Belotserkovskii, O.M., Ed., Moscow: Izd-vo VTs AN SSSR, 1967, pp. 1–400.
14. Spreiter, J.R. and Stahara, S.S., The Location of the Planetary Bow Shocks: A Critical Overview of Theory and Observations, *Adv. Space. Res.*, 1995, vol. 15, p. (8/9)433.
15. Spreiter, J.R., Summers, A.L., and Rizzi, A.W., Solar Wind Flow Past Nonmagnetic Planets—Venus and Mars, *Planet. Space Sci.*, 1970, vol. 18, p. 1281.
16. Slavin, J., Verigin, M., Gringauz, K., *et al.*, The Solar Wind Interaction with Mars: Phobos-2 Bow Shock Observations on 24 March 1989, in *Plasma Environments of Non-Magnetic Planets. COSPAR Colloq. Ser., vol. 4*, Gombosi, T.I., Ed., Tarrytown, N.Y.: Pergamon, 1993, p. 279.
17. Russell C.T. and Zhang T.-L. Unusually Distant Bow Shock Encounters at Venus *Geophys. Res. Lett.*, 1992, vol. 19, p. 833.